PCT

WORLD INTELLECTUAL PROPERTY ORGANIZATION
International Bureau

INTERNATIONAL APPLICATION PUBLISHED UNDER THE PATENT COOPERATION TREATY (PCT)

(51) International Patent Classification 5 :
H01Q 15/00, 13/02, H01P 3/12

A1

(11) International Publication Number: WO 94/00892

(43) International Publication Date: 6 January 1994 (06.01.94)

(21) International Application Number: PCT/GB92/01173

(22) International Filing Date: 29 June 1992 (29.06.92)

(71) Applicant *(for all designated States except US)*: LOUGHBOROUGH UNIVERSITY OF TECHNOLOGY [GB/GB]; Loughborough, Leicestershire LE11 3TF (GB).

(72) Inventors; and
(75) Inventors/Applicants *(for US only)* : VARDAXOGLOU, John, Costas [GB/GB]; 63 William Street, Loughborough, Leicestershire LE11 3BX (GB). SEAGER, Robert, Dennis [GB/GB]; 6 Linden Road, Loughborough, Leicestershire LE11 1PG (GB). ROBINSON, Alan, John [GB/GB]; 30 New Street, Hepthorne Lane, North Wingfield, Chesterfield, Derbyshire S42 5JW (GB).

(74) Agents: RAYNOR, Simon, Mark et al.; Abel & Imray, Northumberland House, 303-306 High Holborn, London WC1V 7LH (GB).

(81) Designated States: JP, US, European patent (AT, BE, CH, DE, DK, ES, FR, GB, GR, IT, LU, MC, NL, SE).

Published
With international search report.

(54) Title: A WAVEGUIDE AND AN ANTENNA INCLUDING A FREQUENCY SELECTIVE SURFACE

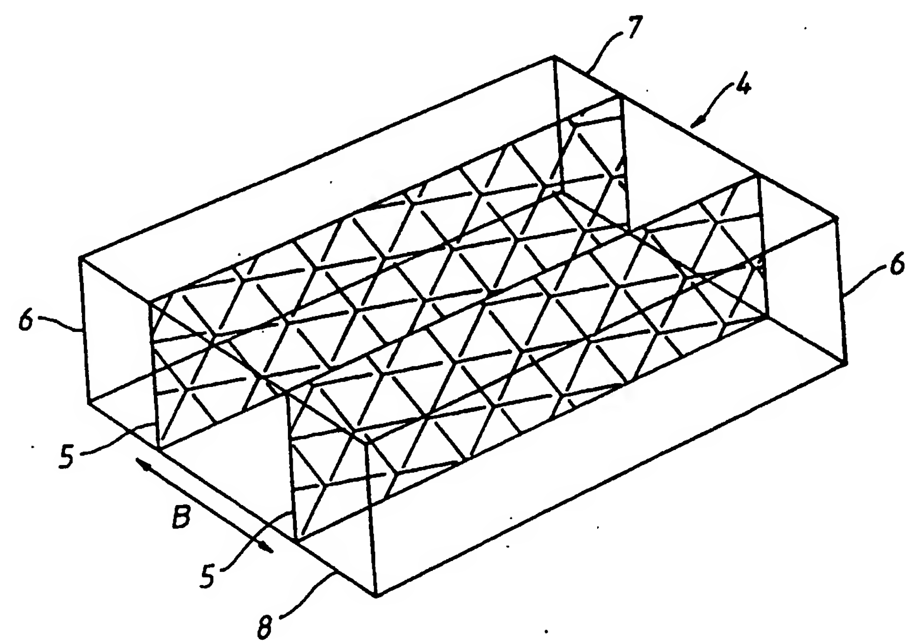

(57) Abstract

A waveguide (4) includes two frequency selective surfaces (5) mounted within the waveguide parallel to its side walls (6). The frequency selective surfaces (5) influence the frequency response of the waveguide (4).

FOR THE PURPOSES OF INFORMATION ONLY

Codes used to identify States party to the PCT on the front pages of pamphlets publishing international applications under the PCT.

AT	Austria
AU	Australia
BB	Barbados
BE	Belgium
BF	Burkina Faso
BG	Bulgaria
BJ	Benin
BR	Brazil
BY	Belarus
CA	Canada
CF	Central African Republic
CG	Congo
CH	Switzerland
CI	Côte d'Ivoire
CM	Cameroon
CN	China
CS	Czechoslovakia
CZ	Czech Republic
DE	Germany
DK	Denmark
ES	Spain
FI	Finland
FR	France
GA	Gabon
GB	United Kingdom
GN	Guinea
GR	Greece
HU	Hungary
IE	Ireland
IT	Italy
JP	Japan
KP	Democratic People's Republic of Korea
KR	Republic of Korea
KZ	Kazakhstan
LI	Liechtenstein
LK	Sri Lanka
LU	Luxembourg
LV	Latvia
MC	Monaco
MG	Madagascar
ML	Mali
MN	Mongolia
MR	Mauritania
MW	Malawi
NE	Niger
NL	Netherlands
NO	Norway
NZ	New Zealand
PL	Poland
PT	Portugal
RO	Romania
RU	Russian Federation
SD	Sudan
SE	Sweden
SI	Slovenia
SK	Slovak Republic
SN	Senegal
TD	Chad
TG	Togo
UA	Ukraine
US	United States of America
UZ	Uzbekistan
VN	Viet Nam

A waveguide and an antenna including a frequency selective surface.

The present invention relates to a waveguide including a frequency selective surface and an antenna including a frequency selective surface. More specifically, the invention relates to a tuneable multiband/ broadband wave guiding system and aperture antenna.

Waveguides and antennas for electromagnetic radiation are generally designed to operate at one specific frequency or within a narrow frequency band. The aim of the present invention is to provide a waveguide and an antenna that have broad or multiple operating frequency bands. It is a further aim of the invention to provide a waveguide and an antenna that are tuneable to operate at different frequencies.

According to the present invention, there is provided a waveguide including a frequency selective surface, the frequency selective surface being arranged to influence the frequency response of the waveguide.

A frequency selective surface (FSS) is an array of antenna elements that acts as a passive electromagnetic filter. The surface may comprise an array of electrically conductive elements on a dielectric substrate or, alternatively, a plurality of apertures in a conductive surface. Electromagnetic waves incident on a surface comprising an array of conductive elements are reflected from the surface only in a narrow band of frequencies and

are transmitted at other frequencies. With an array of apertures, electromagnetic waves are transmitted only in a narrow band of frequencies. Such surfaces are used as multiplexers or radomes in communications systems and can operate at microwave frequencies, including mm-waves, up to infrared and optical frequencies.

At least one frequency selective surface may be mounted within the waveguide, to divide the waveguide longitudinally into two or more parts. Preferably, the frequency selective surface is parallel to a side wall thereof. Mounting a frequency selective surface within a waveguide allows the effective dimensions of the waveguide to vary with the operating frequency, thereby providing broad or multiple operating frequency bands.

Alternatively, the frequency selective surface may be provided over an open end of the waveguide.

The present invention further provides an antenna for microwave radiation, comprising a outer horn and an inner horn, wherein at least the inner horn includes a frequency selective surface. The outer horn or horns may also comprise frequency selective surfaces.

The frequency selective surface may be either reconfigurable of non-reconfigurable. Non-reconfigurable frequency selective surfaces are designed to operate in a particular frequency range, which is determined by the size and the arrangement of the antenna elements and the size of the array. The operating frequency of a non-reconfigurable frequency selective surface cannot be

changed.

A reconfigurable fr quency selective surface comprises at least two arrays of elements, the arrays being arranged in close proximity with one another so that elements of a first array are closely coupled with elements of a second array adjacent to the first array. The first array is displaceable with respect to the second array to adjust the frequency response of the surface.

The first and second arrays may be substantially parallel with one another.

The array elements may be conductive elements on a dielectric substrate, or apertures in a conductive substrate, or a combination of the above.

The first and second arrays may have a separation of no more than 0.03 wavelengths, and preferably no more than 0.003 wavelengths of the electromagnetic waves having the resonant frequency of the surface. For example, when microwaves of frequency 30GHz are to be reflected, the separation is advantageously no more than 0.225mm and preferably no more than 0.025mm.

The first array may be displaceable relative to the second array in a direction parallel to the surfaces of the arrays. Alternatively, the frequency selective surface may be reconfigured by rotating the first array with respect to the second array, or by altering the distance and/or the medium separating the first array from the second array. Using that configuration, there

is no limit to the distance separating the arrays.

The array elements may be parallel linear dipoles, and the at least one array may be displaceable in the longitudinal direction of the linear dipoles.

Embodiments of the invention will now be described, by way of example, with reference to the accompanying drawings, of which:

Figure 1 is a perspective view of a reconfigurable frequency selective surface;
Figure 2 is a cross-section through the surface;
Figure 3 is a diagrammatic view of a part of the surface;
Figure 4 shows the frequency response of a frequency selective surface;
Figure 5 shows the variation of the frequency response as the surface is reconfigured;
Figure 6 shows a waveguide including a frequency selective surface;
Figure 7 shows a prototype waveguide, used for testing its transmission response;
Figures 8 and 9 show the transmission response of the prototype waveguide, and
Figures 9 and 10 show two forms of horn antenna employing frequency selective surfaces.

As shown in figure 6, the waveguide 4 has a rectangular cross-section and includes upper and lower walls 7,

8 and two side walls 6. Two frequency selective surfaces 5 are mounted parallel to its two side walls 6. The frequency selective surfaces 5 divide the waveguide longitudinally into two portions, an inner portion being defined by the upper and lower walls 7, 8 and the frequency selective surfaces 5, and an outer portion being defined by the upper and lower walls 7, 8 and the side walls 6.

The frequency selective surfaces 5 are arranged to transmit at low frequencies and to reflect at higher frequencies. The surfaces 5 are then invisible to the electromagnetic waves in the lower frequency band, and the effective internal dimensions of the waveguide 4 are defined by the side walls 6 and the upper and lower walls 7, 8 of the waveguide 4. At higher frequencies, the frequency selective surfaces 5 will reflect the electromagnetic waves, and the effective internal dimensions of the waveguide 4 will then be defined by the frequency selective surfaces 5 and the upper and lower walls 7, 8 of the waveguide. The effective dimensions of the waveguide are therefore different for different frequencies of transmitted electromagnetic wave, so increasing the operating frequency range of the waveguide.

The operating frequency range of the waveguide is defined at its lower end by the cut-off frequency in the outer waveguide of the dominant TE_{10} propagation mode, and at its upper end by the upper limit of the band-stop

range (i.e. the reflection band) of the frequency selective surface.

Since electromagnetic waves at the upper end of the operating frequency range are reflected by the frequency selective surfaces and confined within the inner waveguide, the higher order modes of the outer waveguide are effectively suppressed. The waveguide therefore permits monomode propagation at the TE_{10} mode over a wide frequency range.

If the reflection coefficient of the frequency selective surfaces is -1 (the ideal value), the group and phase velocities of the high frequency signal in the inner waveguide and the low frequency signal in the outer waveguide will be the same. In practice, although this is approximately true at the centre of the range of operating frequencies, the phase and amplitude of the signals will deviate at other frequencies. This causes the apparent positions of the frequency selective surfaces to vary with frequency. By providing double- or multi-layer frequency selective surfaces, the apparent positions of the frequency selective surfaces may be made to move inwards with increasing frequency, thereby providing a non-dispersive waveguide of even greater bandwidth.

By using reconfigurable frequency selective surfaces, which are described below with reference to figures 1 to 5, the operating frequency of the waveguide may be controlled electronically. The frequency selec-

tive surfaces, which may be fixed or reconfigurable and either single or multilayer structures, can be used to provide a number of waveguide devices, such as filters, polarisers or phase shifters. The surfaces may be positioned at any location within a waveguide. The reconfigurable frequency selective surfaces may be electronically tuned, the speed of the tuning and the performance of each application being governed by the array design and the process of attaining the reconfigurable frequency selective surface effect.

Figs. 8 and 9 show the results of experimental tests on the waveguides, which demonstrate the principles of operation of the waveguide. The results were obtained using the prototype waveguide shown in Fig. 7, which consists of a standard X-band waveguide from which the narrow side walls have been removed. The waveguide comprises broad upper and lower conducting walls 9, 10 having on their inner faces several longitudinal slots 11 into which frequency selective surfaces can be inserted.

The transmission response of the prototype in the X band (8-12.4 GHz) is shown in Fig. 8. When operated without any inserts, the prototype exhibits a moderately lossy transmission band from the cut-off frequency up to about 16GHz. Placing radar-absorbing material (RAM) along the lengths of the open sides of the waveguide increases insertion loss dramatically in the X-band, showing that fringing fields exist outside the waveguide when operated in this mode. When frequency selective

surfaces are placed in the outer slots of the waveguide (giving it the same transverse cross-section as the X-band waveguide, improved transmission is provided over the 14 to 16 GHz range, which corresponds to the reflection band of the frequency selective surfaces. Introducing the RAM with the frequency selective surfaces in place produces little disturbance to this high frequency band whilst the lower frequencies are attenuated by more than 50 dB. The frequency selective surfaces therefore clearly contain waves in the higher frequency range. The nulls seen at about 14.5 and 16.6 GHz are believed to be due to higher order modes caused by the poor performance of the transitions at this frequency.

Fig. 9 shows the results of a similar set of measurements carried out with J-band (12.4-18 GHz) transitions attached to each end of the test prototype. The separation of the frequency selective surfaces was equal to the width dimension of a standard J-band waveguide. The guiding effect of the frequency selective surfaces is again displayed. The design of an integrated transition incorporating frequency selective surfaces enables tuneable broadband waveguide designs to be operated with a single co-axial feed at all frequencies. The null observed near to 13GHz is due to a filtering effect caused by the frequency selective surface elements and the varying positions of the electrical walls. A reconfigurable frequency selective surface would enable a band-stop or a band-pass filtering response to be tuned.

As shown in Fig. 9, similar results to those produced in the frequency selective surface/open wall case were produced when frequency selective surfaces were inserted into a standard X-band waveguide. The close proximity of the copper wall of the waveguide to the frequency selective surfaces does not significantly modify their guiding effect. The figure also shows the calculated reflection coefficient amplitude for a single layer large array of tripoles over the range 13 to 18 GHz. The array used in the waveguide was a single line of tripole elements. The reflection band of the large frequency selective surface is broadly similar to the enhanced transmission range measured in the test prototype. The frequency selective surface reflection coefficients were calculated using a Floquet mode analysis, assuming that the finite line array of tripoles behaves as an infinite rectangular lattice array with vertical periodicity equal to the waveguide height. The calculations also assumed a nominal incidence angle of 30° from normal (a reasonable approximation to the varying angles of incidence in the waveguide), to account for the oblique nature of the plane waves which may be used to describe the fields in the waveguide for the TE_{10} mode.

A broadband/multiband antenna, which operates according to the same principles as the waveguide described above, is shown in Figs. 10 and 11. Fig. 10 shows a broadband pyramidal horn antenna having an outer

horn 12 of conducting material and an inner horn 13, formed of fixed or reconfigurable frequency selective surfaces. The frequency selective surfaces are invisible to electromagnetic signals of low frequency, which therefore occupy the outer horn, whereas signals of higher frequency are confined within the inner horn. The effective dimensions of the antenna therefore vary with the operating frequency, allowing it to operate over a wide frequency range.

Fig. 11 shows an alternative antenna comprising two co-axial cones 14, 15, both consisting of fixed or reconfigurable frequency selective surfaces. The antenna can be tuned to a specific frequency band for improved performance and for matching to a waveguide of the type described above. The walls of the outer cone 14 could be replaced by conducting walls if band tuning and/or antenna matching is not required. If desired, the antenna may include more than two cones.

As shown in figure 1, a reconfigurable frequency selective surface consists of two parallel arrays 1, 2 of elements 3. The array elements 3 may be either electrically conductive elements, such as dipoles, printed on a dielectric substrate, or apertures, such as slots, formed in a conductive surface (Babinet's compliment of the former). A non-reconfigurable frequency selective surface consists simply of just one of the arrays 1, 2 shown in figure 1.

The two arrays 1,2 are arranged in close proximity

with one another, so that the elements 3 of the first array 1 are closely coupl d with the elements of the second array 2. The separation S of the arrays is as small as possible, whilst ensuring that the elements of the first array 1 are electrically insulated from the elements of the second array 2, and will generally be of the order of 0.03 wavelengths or less, although this will depend on the particular array design, and the dielectric constant of the substrate.

The second array 2 is displaceable relative to the first array 1 by a small distance DS. In the embodiment shown in figure 1, the second array 2 can be displaced transversely, parallel to the surfaces of the arrays, in the direction of the Y-axis. Other types of displacement are, however, possible: for example, the second array 2 could be displaced in the direction of the X-axis or the Z-axis (thereby altering the distance S separating the two arrays) or it could be rotated about the Z-axis, or displaced in any combination of those directions.

When the arrays 1,2 are aligned accurately with one another (so that DS=0), the elements 3 of the first array 1 lie directly over the elements of the second array 2, thereby shadowing the second array 2 from the incident electromagnetic waves. The frequency response of the surface is then similar to that of a single array which, as shown in figure 4, includes a narrow reflection band and upper and lower transmission bands. The letters f_R denote the reflection band centre frequency, which

corresponds to the resonant frequency of the surface, and the letters f_T denote th frequency of the lower transmission band. The frequencies f_R and f_T of the reflection and transmission bands are determined by the length of the antenna elements 3 and the size of the array.

As shown in figures 2 and 3, the first array 1 has a plurality of elements 3 of length L1, and the second array 2 has a plurality of elements of length L2. The separation D1,D2 and the arrangement of the elements in each of the arrays is similar, so that when DS=0 the elements of the second array 2 lie in the shadows of the elements of the first array 1.

When, as shown in figure 2, the second array 2 is displaced transversely in the direction Y by a distance DS, the ends of the elements 3 of the second array 2 then extend by a small distance DL beyond the ends of the elements of the first array 1. Since the elements of the two arrays are closely coupled, this produces an increase in the overall effective length of each element, which affects the frequency response of the surface. As shown in figure 5, the reflection frequency f_R of the surface is shifted by an amount that is approximately proportional to the displacement DS. The frequency response of the surface can similarly be translated by displacing the second array 2 in the X or Z directions, by rotating it about the Z-axis, or by any combination of those movements.

An example of the results that can be achieved with a particular reconfigurable frequency selective surface will now be described. The particular frequency selective surface consists of two arrays 1,2 of linear dipoles 3, printed in a square lattice on a 0.037mm thick dielectric substrate of dielectric constant 3. The geometry of the lattice unit cell is shown in figure 3, wherein L represents the length of the antenna element, W the element's width, and D the side length of the unit cell (equal to the separation of adjacent antenna elements). In the first array 1, L=4.3mm, W=0.4mm and D=6mm. In the second array 2, L=3.25mm, W=0.4mm and D=6mm. Each array is square, having sides of length 20cm, and the separation S between the arrays is about 0.225mm.

The measured and theoretical response of the surface to microwaves of frequency 12-40GHz at both normal incidence and a TE incidence of 45^{o}, with the electric field parallel to the dipoles, is shown in figure 5. By comparison, the variation in the frequency response of a single array with increasing dipole length is shown as a solid line at the top of the graph.

When the two arrays are substantially aligned, with DS in the range 0 to 0.625mm, the frequency response of the surface is similar to that of a single array having the dimensions and lattice arrangement of the first array 1. Resonance takes place at frequencies of about 31GHz and 27GHz for normal and TE:45^{o} states of incidence

respectively. A frequency shift takes place as the transverse displacement DS of the second array 2 is increased, maximum measured frequency shifts of 36% and 22% for normal and TE:45^o states of incidence respectively being achieved at a displacement of DS=3mm. At that displacement, the elements 3 of the second array 2 completely fill the gaps between the elements of the first array 1, and so a further increase in the displacement DS has no further effect on the frequency response of the surface.

Reducing the separation S of the arrays, thereby increasing the coupling between the elements, allows greater frequency shifts to be achieved. For example, with a separation of 0.025mm, frequency shifts of up to 60% can theoretically be obtained. The theoretical frequency shift at a separation S of 0.025mm is also shown in figure 5. There is no deterioration in the band widths or band spacing ratio (f_R/f_T) of the surface as the displacement increases and the response of the surface is therefore stable throughout the frequency range.

Various modifications of the apparatus described above are, of course, possible. Many different array geometries could be used and each array may consist either of a plurality of conductors on a dielectric substrate, or a perforated plate, or a combination of both. The antenna el ments may be dipoles, cross-dipoles, tripoles, Jerusalem crosses, squares, open-ended

loops or any other type of antenna element. The elements need not necessarily be arranged periodically and the arrays may be planar or curved. The frequency selective surface may further consist of two or more closely-coupled arrays of elements, and the respective arrays may either be displaced in a direction parallel to the surfaces of the arrays, or rotated or their separation altered, or the medium separating the arrays may be adjusted (for example, by adjusting its dielectric constant).

The relative displacement of the two arrays may be controlled in various different ways. For example, piezoelectric actuators can be used to control the precise relative movement of the arrays, and the arrays can be printed directly onto the piezoelectric material. The frequency selective surface may have piezoelectric actuators positioned at some sub-areas of its surface, i.e. not everywhere on its surface. Alternatively, the arrays can be mounted at a small separation and air pumped from the gap between the arrays to alter their separation.

Claims:

1. A waveguide including a frequency selective surface, the frequency selective surface being arranged to influence the frequency response of the waveguide.

2. A waveguide according to claim 1, in which at least one frequency selective surface is mounted within the waveguide to divide the waveguide longitudinally into two or more parts.

3. A waveguide according to claim 2, in which the frequency selective surface is parallel to a wall of the waveguide.

4. A waveguide according to claim 3, in which two frequency selective surfaces are mounted within the waveguide, parallel to the side walls thereof.

5. A waveguide according to any one of the preceding claims, in which the frequency selective surface is a reconfigurable frequency selective surface.

6. A waveguide according to claim 5, in which the reconfigurable frequency selective surface comprises at least two arrays of elements, the arrays being arranged in close proximity with one another so that elements of a first array are closely coupled with elements of a second array adjacent to the first array, the first array being

displaceable with respect to the second array to adjust the frequency response of the surface.

7. An antenna for microwave radiation, comprising a outer horn and an inner horn, wherein the inner horn includes a frequency selective surface.

8. An antenna according to claim 7, in which the outer horn includes a frequency selective surface.

9. An antenna according to claim 7 or claim 8, in which the inner and outer horns are coaxial.

10. An antenna according to any one of claims 7 to 9, in which the horns have a rectangular transverse cross-section.

11. An antenna according to any one of claims 7 to 9, in which the horns have a circular transverse cross-section.

12. An antenna according to any one of claims 7 to 11, in which at least one frequency selective surface is a reconfigurable frequency selective surface.

13. A waveguide according to claim 1, in which a frequency selective surface is provided over an open end of the waveguide.

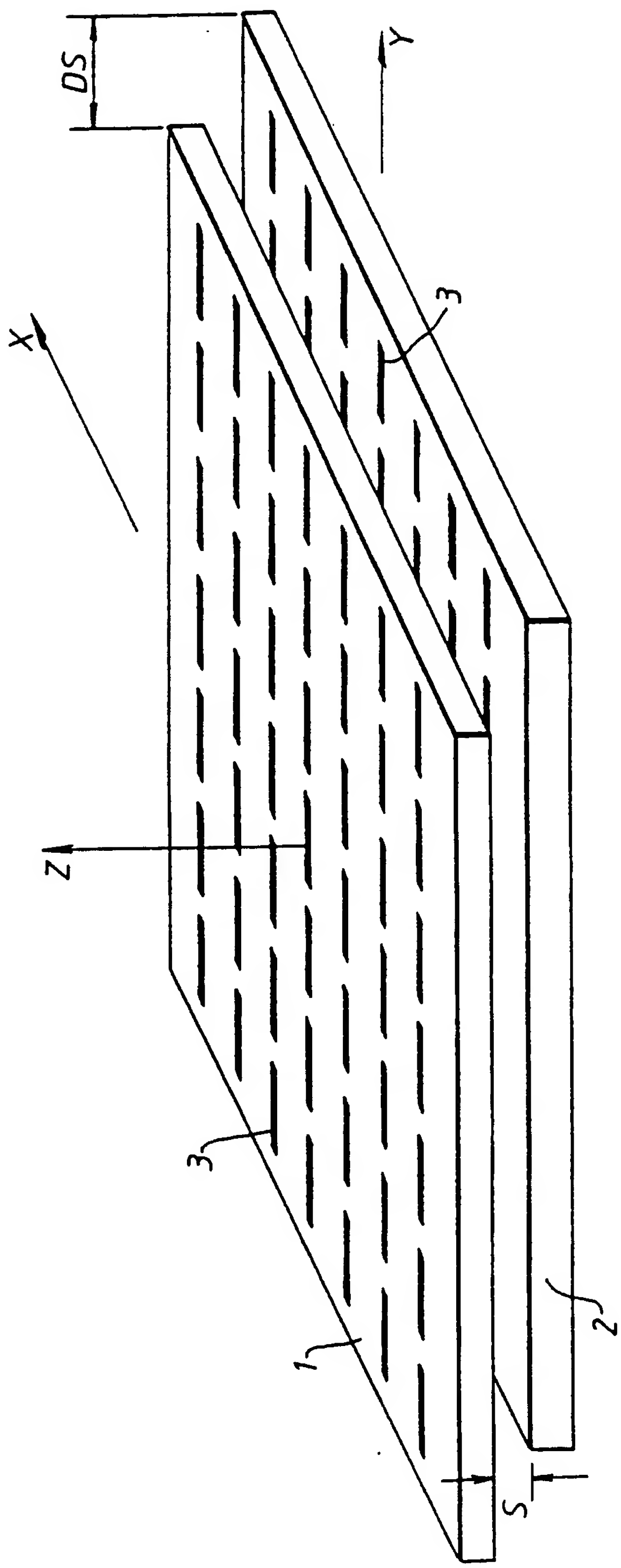

Fig.1.

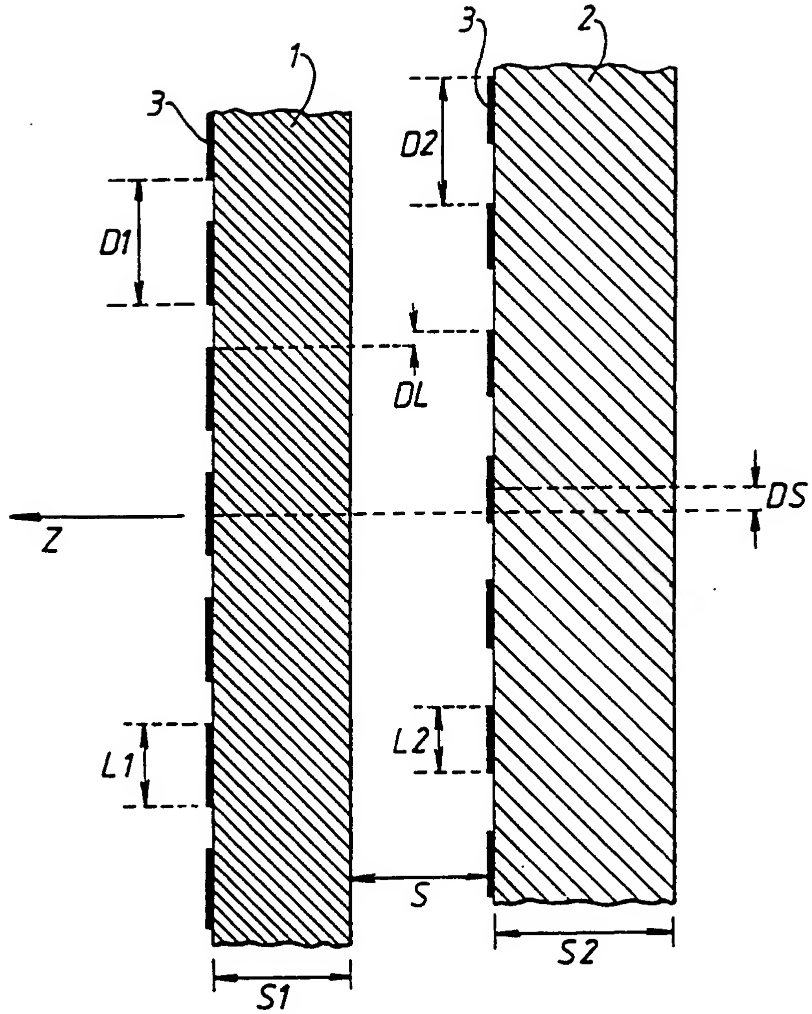

Fig.2.

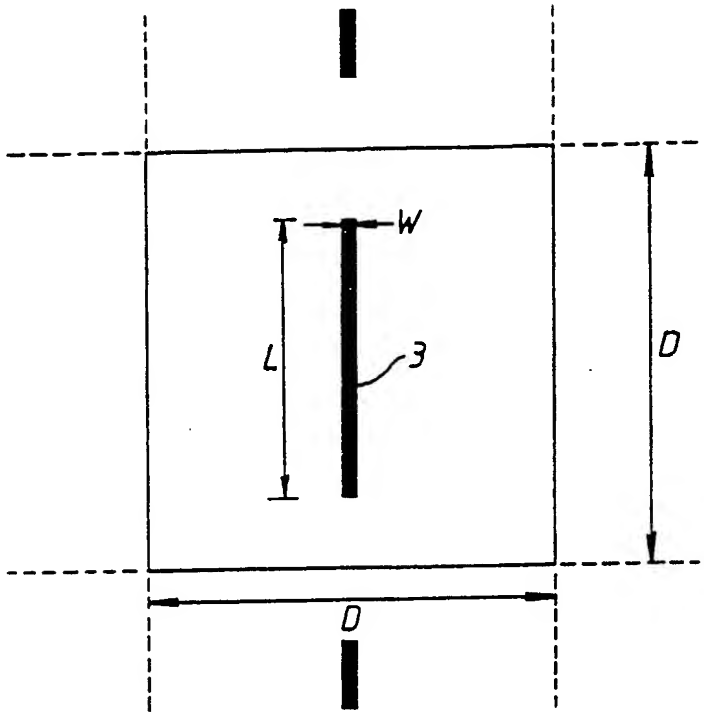

Fig. 3.

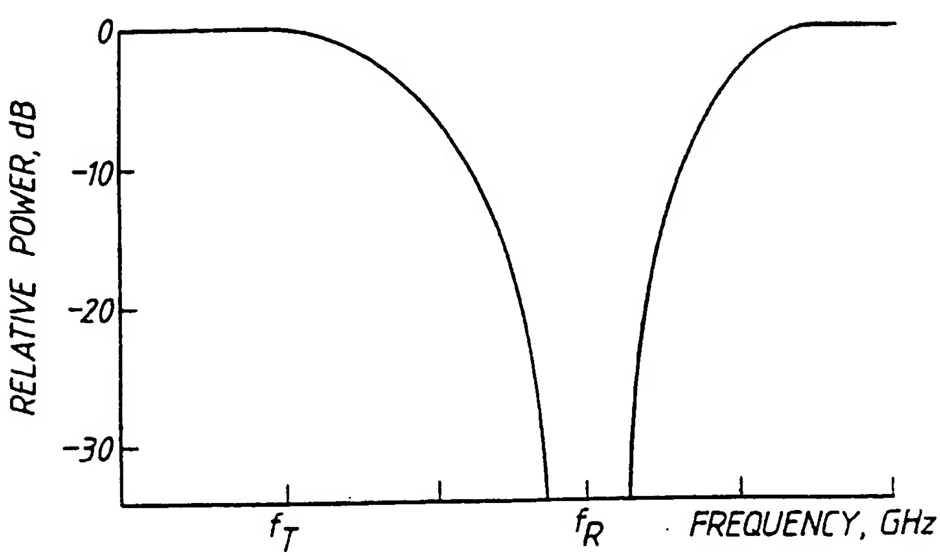

Fig. 4.

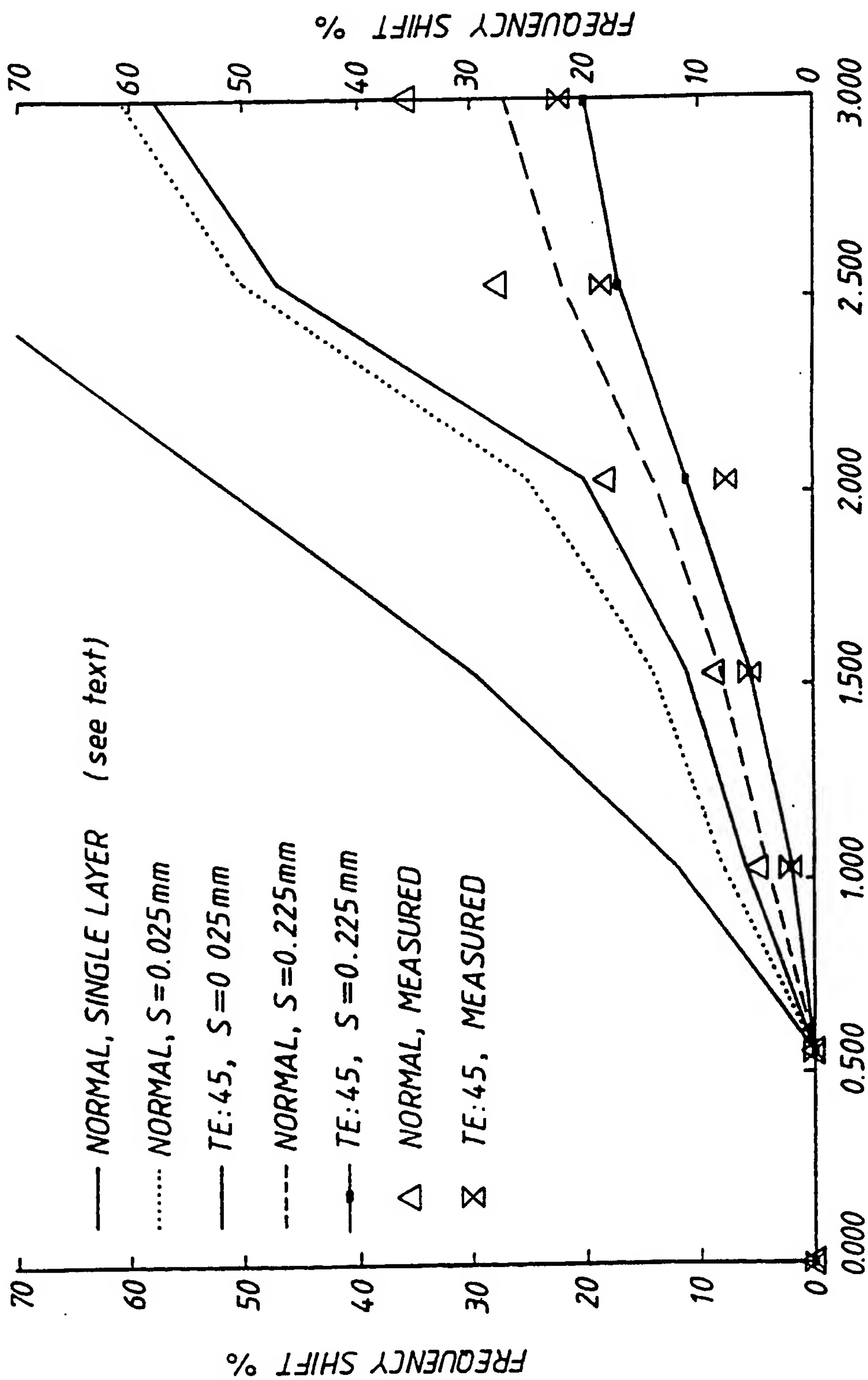
NORMAL, SINGLE LAYER (see text)
NORMAL, S=0.025mm
TE:45, S=0 025mm
NORMAL, S=0.225mm
TE:45, S=0.225mm
NORMAL, MEASURED
TE:45, MEASURED
FREQUENCY SHIFT %
0
10
20
30
40
50
60
70
0.000
0.500
1.000
1.500
2.000
2.500
3.000
DS mm

Fig.5.

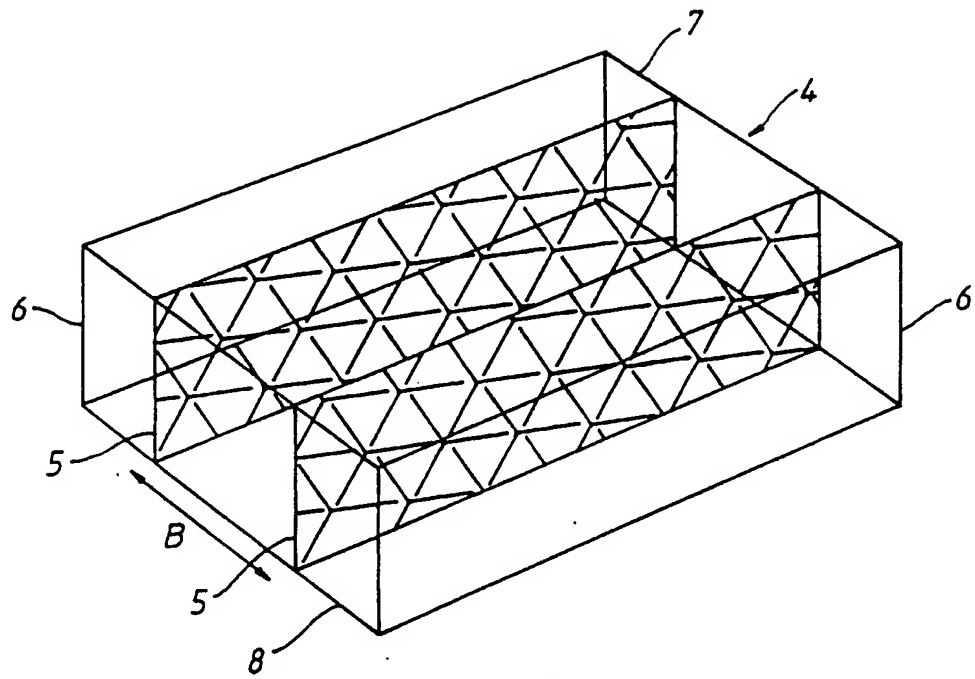

Fig.6.

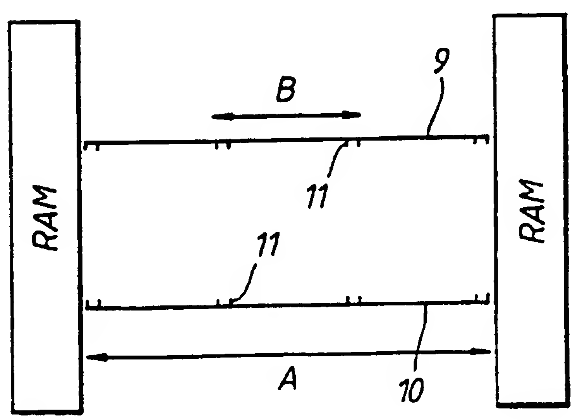

Fig.7.

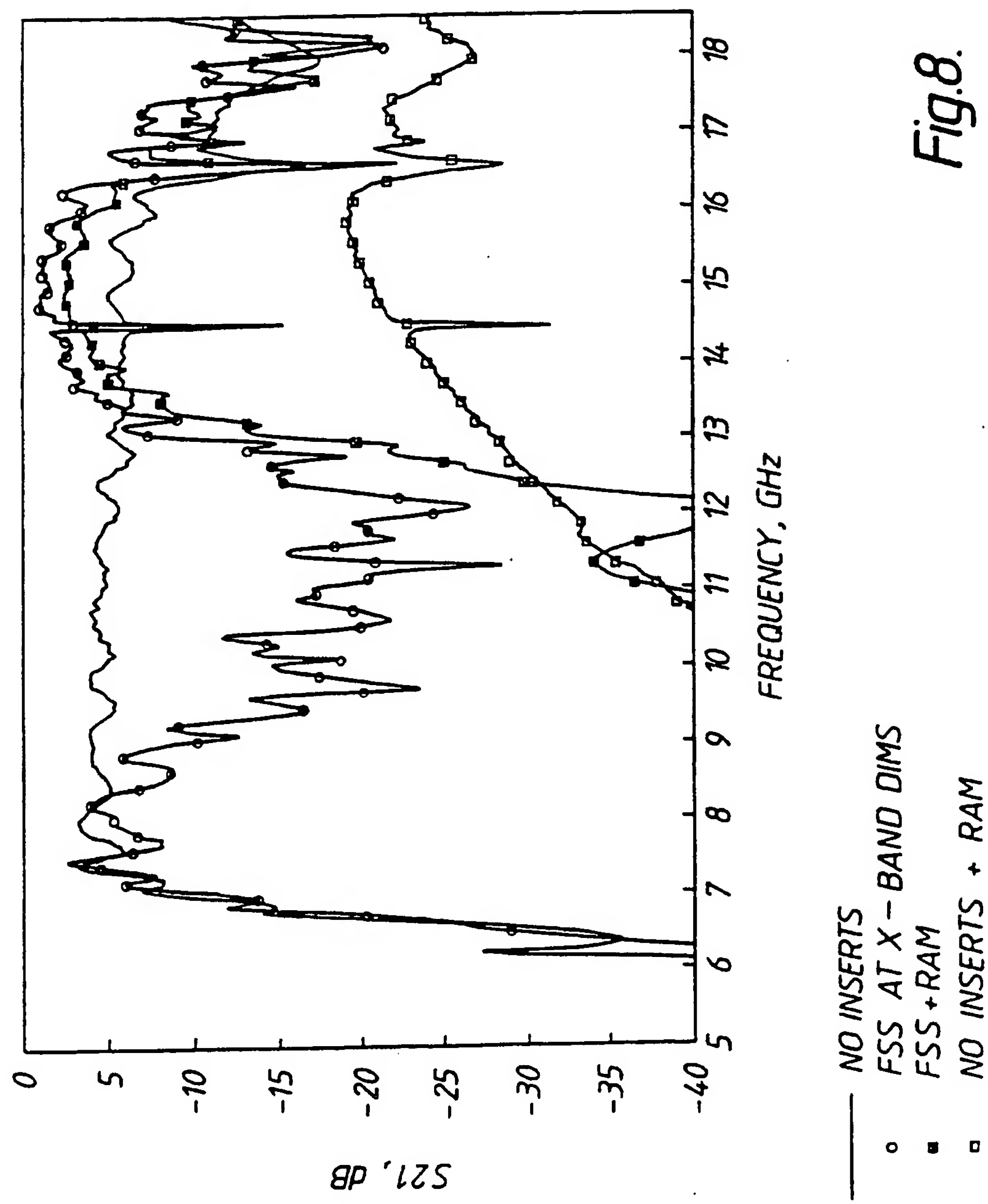
S21, dB
0
-5
-10
-15
-20
-25
-30
-35
-40
5
6
7
8
9
10
11
12
13
14
15
16
17
18
FREQUENCY, GHz
NO INSERTS
FSS AT X-BAND DIMS
FSS+RAM
NO INSERTS + RAM

Fig.8.

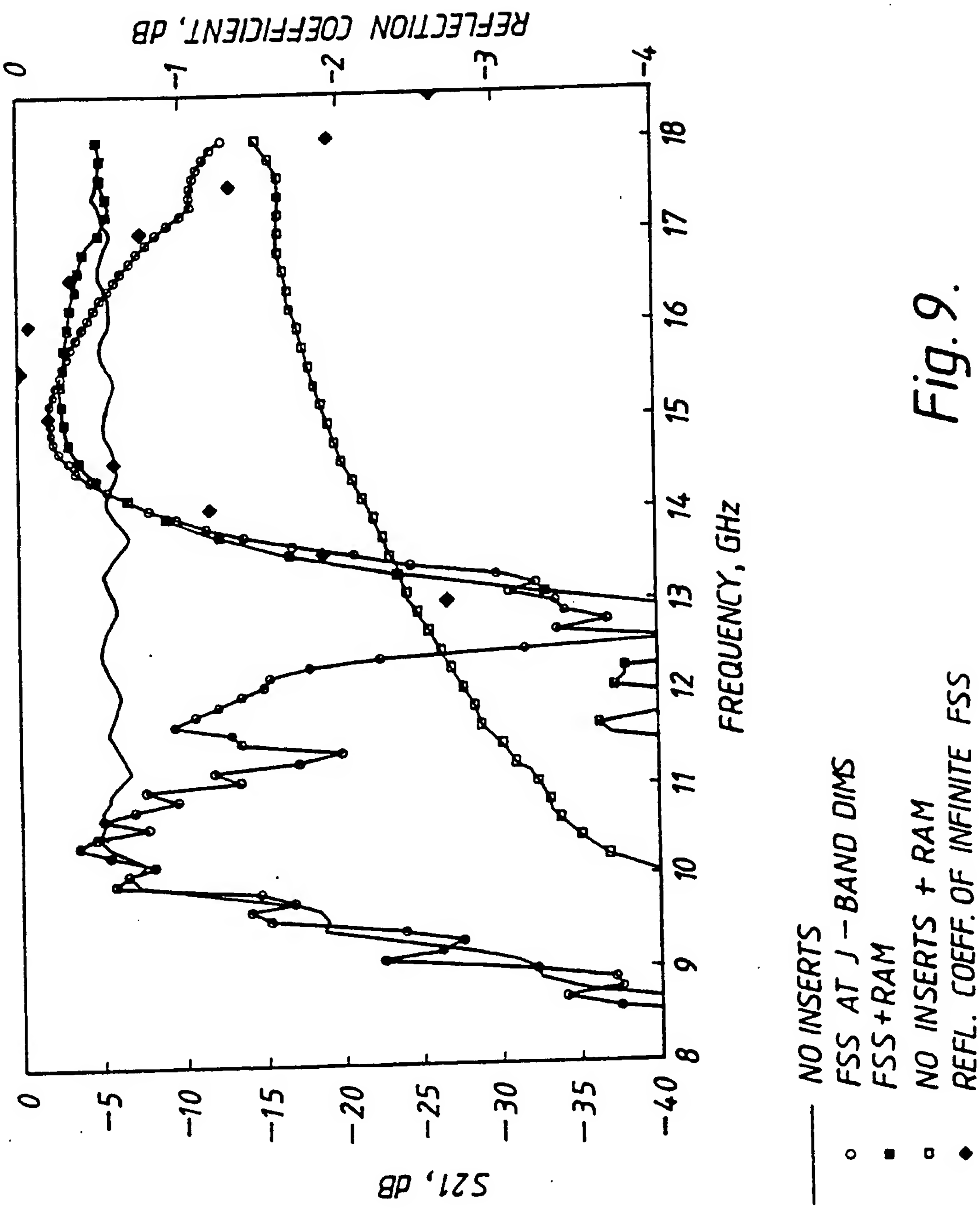
REFLECTION COEFFICIENT, dB
0
-1
-2
-3
-4
S21, dB
0
-5
-10
-15
-20
-25
-30
-35
-40
FREQUENCY, GHz
8
9
10
11
12
13
14
15
16
17
18
NO INSERTS
FSS AT J-BAND DIMS
FSS+RAM
NO INSERTS + RAM
REFL. COEFF. OF INFINITE FSS

Fig. 9.

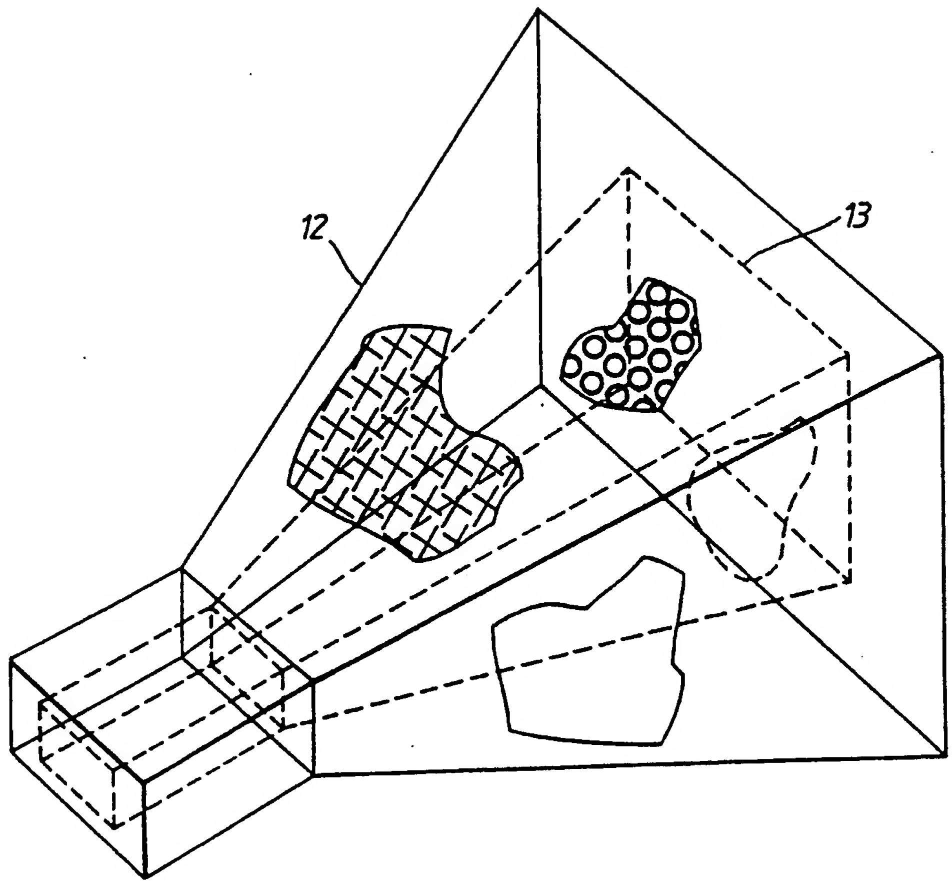

Fig.10.

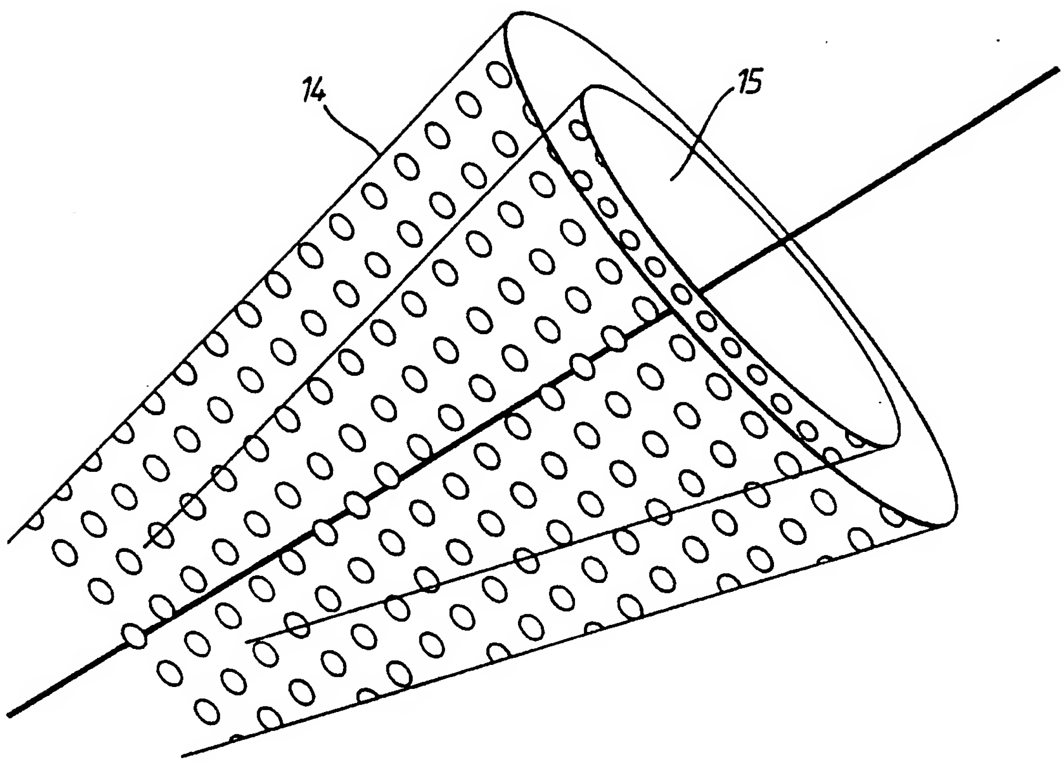

Fig.11.

INTERNATIONAL SEARCH REPORT

International Application No PCT/GB 92/01173

I. CLASSIFICATION OF SUBJECT MATTER (if several classification symbols apply, indicate all)[6]

According to International Patent Classification (IPC) or to both National Classification and IPC

Int.Cl. 5 H01Q15/00; H01Q13/02; H01P3/12

II. FIELDS SEARCHED

Minimum Documentation Searched[7]

Classification System	Classification Symbols
Int.Cl. 5	H01Q ; H01P

Documentation Searched other than Minimum Documentation to the Extent that such Documents are Included in the Fields Searched[8]

III. DOCUMENTS CONSIDERED TO BE RELEVANT[9]

Category °	Citation of Document, [11] with indication, where appropriate, of the relevant passages [12]	Relevant to Claim No.[13]
X	US,A,3 633 206 (MCMILLAN) 4 January 1972 see column 3, line 1 - line 46 see column 10, line 8 - line 54; figures 1,3A,B	1,13
X	PATENT ABSTRACTS OF JAPAN vol. 014, no. 584 (E-1018)27 December 1990 & JP,A,22 54 801 (MIYATA YOSHIHIDE) see abstract	7
A	US,A,4 028 650 (KONISHI ET AL.) 7 June 1977 see claims 1-5; figures 1-17	1-6
	-/--	

° Special categories of cited documents : [10]

"A" document defining the general state of the art which is not considered to be of particular relevance

"E" earlier document but published on or after the international filing date

"L" document which may throw doubts on priority claim(s) or which is cited to establish the publication date of another citation or other special reason (as specified)

"O" document referring to an oral disclosure, use, exhibition or other means

"P" document published prior to the international filing date but later than the priority date claimed

"T" later document published after the international filing date or priority date and not in conflict with the application but cited to understand the principle or theory underlying the invention

"X" document of particular relevance; the claimed invention cannot be considered novel or cannot be considered to involve an inventive step

"Y" document of particular relevance; the claimed invention cannot be considered to involve an inventive step when the document is combined with one or more other such documents, such combination being obvious to a person skilled in the art.

"&" document member of the same patent family

IV. CERTIFICATION

Date of the Actual Completion of the International Search	Date of Mailing of this International Search Report
26 FEBRUARY 1993	05. 03. 93
International Searching Authority	**Signature of Authorized Officer**
EUROPEAN PATENT OFFICE	ANGRABEIT F.F.K.

III. DOCUMENTS CONSIDERED TO BE RELEVANT (CONTINUED FROM THE SECOND SHEET)		
Category °	Citation of Document, with indication, where appropriate, of the relevant passages	Relevant to Claim No.
A	GB,A,600 433 (BOOKER) 8 April 1948 see page 1, left column, line 21 - right column, line 87; figures 1-6 ---	7-13
A	US,A,3 028 565 (WALKER ET AL.) 3 April 1962 see claims 1,2; figure 2 ---	1-4
A	EP,A,0 468 623 (BRITISH AEROSPACE) 29 January 1992 see abstract see column 4, line 19 - line 39 see column 5, line 4 - line 18; figures 1,2 ---	1,5,7,12
E	GB,A,2 253 519 (LOUGHBOROUGH UNIVERSITY OF TECHNOLOGIE) 9 September 1992 see the whole document -----	1-13

ANNEX TO THE INTERNATIONAL SEARCH REPORT ON INTERNATIONAL PATENT APPLICATION NO.

GB 9201173
SA 61615

This annex lists the patent family members relating to the patent documents cited in the above-mentioned international search report.
The members are as contained in the European Patent Office EDP file on 26/02/93
The European Patent Office is in no way liable for these particulars which are merely given for the purpose of information.

Patent document cited in search report	Publication date	Patent family member(s)		Publication date
US-A-3633206	04-01-72	None		
US-A-4028650	07-06-77	JP-C-	1189354	13-02-84
		JP-A-	49010648	30-01-74
		JP-B-	58003401	21-01-83
		AU-A-	5597073	28-11-74
		CA-A-	977049	28-10-75
		DE-A,B	2326331	29-11-73
		FR-A,B	2185866	04-01-74
		GB-A-	1438149	03-06-76
		NL-A-	7307150	27-11-73
		US-A-	3914713	21-10-75
GB-A-600433		None		
US-A-3028565		None		
EP-A-0468623	29-01-92	None		
GB-A-2253519	09-09-92	None		

For more details about this annex : see Official Journal of the European Patent Office, No. 12/82

the velocity of light in free space and x_{01} is a constant whose value depends on the ratio b/a only if the value of ε_r is quite high [4] ($\varepsilon_r > \sim 20$). The bandwidth of the antenna, which is inversely proportional to the radiation Q-factor of the mode, also depends on the parameters ε_r, d/a and b/a. However, its computation is quite complicated.

Experimental results: A dielectric ring resonator with parameters $\varepsilon_r = 36{\cdot}2$, $2a = 11{\cdot}95$ mm, $d = 5{\cdot}4$ mm and $b/a = 0{\cdot}17$ was chosen for experiments. For the chosen value of b/a, the value of x_{01} was found to be 4·24 [4]. Substituting the value of x_{01} and the other parameters in eqn. 1, the frequency of resonance is found to be 6·09 GHz. The return loss of the antenna fed by a probe of length 5·0 mm is shown in Fig. 2. It is seen that the frequency for which the return loss is minimum is very close to the theoretically computed frequency of resonance. The 10 dB bandwidth of the antenna is ~5%. It was found that the impedance bandwidth of the antenna was quite insensitive to the length of the probe which was varied from 3 to 8 mm.

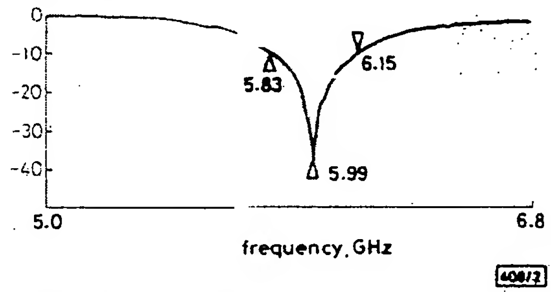

Fig. 2 *Measured return loss of antenna shown in Fig. 1a*
$\varepsilon_r = 36{\cdot}2$, $2a = 11{\cdot}95$ mm, $d = 5{\cdot}4$ mm and $b/a = 0{\cdot}17$

The DR was mounted on a square metallic plane of size $15 \times 15\,\text{cm}^2$. The size of the ground plane is $\sim 3\lambda_0 \times 3\lambda_0$ where λ_0 denotes the wavelength in free space at the centre frequency of the antenna. Because the length of the ground plane is relatively small, it is expected that the radiation pattern of the antenna will be affected by the edges of the ground plane [5]. The measured radiation pattern of the antenna in the E-plane passing through the axis of the resonator is shown in Fig. 3. Although the pattern as shown in Fig. 3 deviates from that of an ideal electric monopole, it is nearly identical to that of a wire electric monopole placed above a finite ground plane of approximately the same size (in terms of wavelengths) [5]. In the H-plane, the measured pattern was found to be nearly circularly symmetric, like that of an ideal monopole.

For the chosen resonator parameters, the height of the antenna is approximately $\lambda_0/10$. It may be remarked that the height of the antenna can be further reduced by choosing a lower aspect ratio ($d/2a$) of the resonator. Also, the bandwidth of the antenna can be further increased by choosing a lower value of ε_r or a larger value of b/a. It is known that the

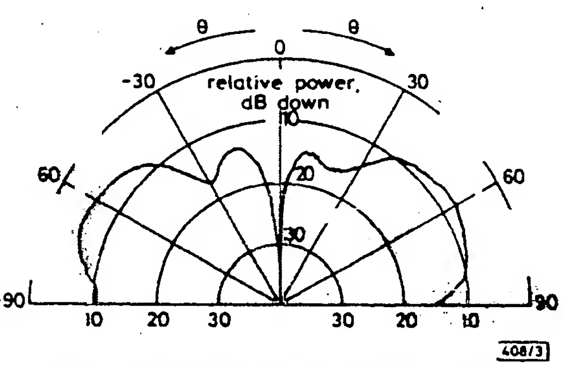

Fig. 3 *Measured elevation plane pattern in upper-half plane of antenna shown in Fig. 1a*
$\varepsilon_r = 36{\cdot}2$, $2a = 11{\cdot}95$ mm, $d = 5{\cdot}4$ mm and $b/a = 0{\cdot}17$

Q-factor of the $TM_{01\delta}$ mode which determines the bandwidth of the antenna is strongly influenced by the resonator parameters [4].

Conclusions: A dielectric resonator antenna designed to radiate like an electric monopole is reported. Initial results show that the proposed configuration is quite promising for constructing small and compact 'electric monopole' antennas.

Acknowledgments: The assistance of M. Lee (Univ. of Ottawa) in the fabrication of the antenna is gratefully acknowledged.

15th June 1993

R. K. Mongia and P. Bhartia (*Department of Electrical Engineering, University of Ottawa, 161 Louis Pasteur, Ottawa, Ontario K1N 6N5, Canada*)

A. Ittipiboon and M. Cuhaci (*Communications Research Center, 3701, Carling Avenue, Ottawa, Ontario K2H 8S2, Canada*)

References

1 LONG, S. A., MCALLISTER, M., and SHEN, L. C.: 'The resonant cylindrical dielectric cavity antenna', *IEEE Trans.*, 1983, AP-31, pp. 406–412

2 MONGIA, R. K.: 'Half-split dielectric resonator placed on a metallic plane for antenna applications', *Electron. Lett.*, 1989, 25, pp. 462–464

3 KISHK, A. A., AHN, B., and KAJFEZ, D.: 'Broad band stacked dielectric resonator antennas', *Electron. Lett.*, 1989, 25, pp. 1232–1233

4 VERPLANKEN, M., and VAN BLADEL, J.: 'The electric-dipole resonances of ring resonators of very high permittivity', *IEEE Trans.*, 1976, MTT-24, pp. 108–112

5 BALANIS, C. A.: 'Antenna theory' (John Wiley, New York, 1982), pp. 502–524

WAVE GUIDANCE AND RADIATION FROM A HOLLOW TUBE FORMED FROM FREQUENCY-SELECTIVE SURFACES

A. J. Robinson, J. C. Vardaxoglou and R. D. Seager

Indexing terms: Frequency-selective surfaces, Waveguides

A hollow tube (rectangular cross-section) employing a frequency selective surface of conducting elements has been constructed and tested as a waveguiding structure. The measured results presented include the frequency response of the waveguide and radiation patterns observed at frequencies away from the guiding region. The important aspects of the results are discussed with reference to fast and slow wave structures.

Introduction: Passive array inserts (such as finite frequency selective surfaces (FSSs)) representing parallel sheets inside standard waveguides have been shown to exhibit wave guidance over the frequency of resonance of the array [1]. Using the same principle, conical frequency selective horns have been constructed and assessed for multiband applications [2]. In this Letter we present the measured behaviour of a guiding structure based on a hollow tube formed entirely from a two-dimensional frequency-selective surface. The tube has rectangular cross-section as in standard rectangular waveguide and hence is termed a frequency-selective guide (FSG) as it has also been observed to exhibit guidance. The propagation in, as well as the radiation from, a prototype FSG of conducting elements printed on a thin dielectric sheet is described.

Construction of tube: The tube, whose cross-section is shown in Fig. 1, was formed by folding a sheet of FSS made by a photolithographic process. The FSS elements were copper concentric square loops printed on a dielectric substrate of thickness 0·1 mm and dielectric constant 3·0. This relatively thick substrate was chosen in order to give the structure some

mechanical strength. The interior of the tube was supported by a former made of low density expanded polystyrene. Because it is not possible to arrange (with constant element size) an integer number of elements on each wall, the prototype was contructed with the centre line of one broad wall as a line of symmetry and the join in the surface required to make a tube was placed on the centre line of the opposing broad wall. Rather than cut through elements to make a butt joint, the elements were left intact and the surface allowed to overlap slightly at the join.

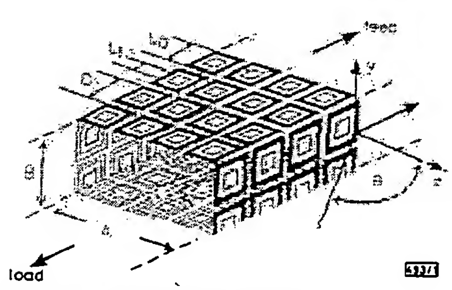

Fig. 1 *Section of frequency selective guide*
$A = 22$ mm, $B = 10$ mm, $D = 5{\cdot}5$ mm, $L_1 = 3{\cdot}1$ mm (width $= 0{\cdot}1$ mm), $L_0 = 5{\cdot}2$ mm (width $= 0{\cdot}3$ mm)

Frequency response results: Fig. 2 shows the measured S_{21} parameter for a 232 mm length of FSG. The structure was fed either end by post and dielectric co-ax to waveguide adaptors. It may be seen that the forward transmission exhibits a peak at 14·5 GHz. This corresponds closely with the predicted and measured FSS planewave transmission minimum at 15 GHz for angles of incidence up to 45°. The maximum level of this forward transmission is 2·5 dB below that observed with standard copper waveguide at this frequency. The loss is believed to be influenced by the non-coincidence of the frequencies of resonance of the broad and narrow walls due to the different incident field conditions on each wall type.

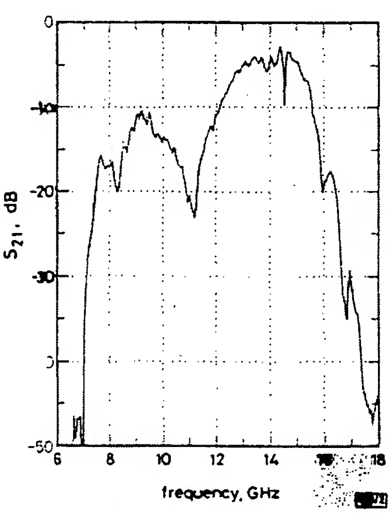

Fig. 2 *Insertion loss of waveguide*

A second transmission maximum occurs well below the FSS resonance at around 9 GHz. This peak appears to be a surface wave bounded to the walls, because it was considerably reduced by placing absorbing material around the exterior of the FSG. This is in contrast to the energy in the upper guiding band which appears to be contained within the guide, resulting in a fast wave structure. Between the two guiding bands a null in the forward transmission is observed. S_{11} measurements on the structure did not reveal a peak in this frequency region. It is therefore inferred that, discarding minor resistive losses, the wave is being leaked in the form of a radiation field. This is discussed in the following Section.

Radiation from FSG structure: For the radiation pattern measurements the FSG was fed at one end by a co-ax to waveguide adaptor and the other end of the structure was matched to a load. Radiation patterns were taken in the $-70 \le \theta \le 80°$ range, centred on broadside for frequencies of 11–22 GHz in 1 GHz steps. The negative angle is taken towards the feed end with the receive probe 1·14 m from the FSG, having the E field parallel to y. It was found that the strongest radiation was measured from the side wall, shown in Fig. 3 for several frequencies. Amplitude is relative to that of a conventional pyramidal horn with a specified gain of 20 dBi. The pattern values were below -22 dB in the negative region, $-70 \le \theta \le 0°$. The maximum beam amplitude occurs at a frequency of 12 GHz, which corresponds to a frequency slightly above the null in the FSG forward transmission response, confirming that power loss here is indeed due to a radiated field. As the frequency is varied away from this value the beam amplitude and direction varies resulting in a frequency scan operation. Similar effects, but with a 10 dB reduction in the levels, have been observed from the top wall of the FSG.

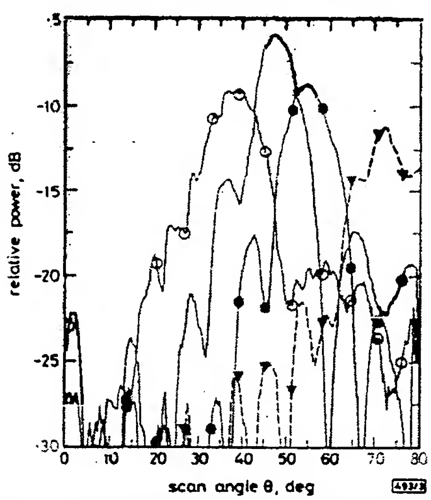

Fig. 3 *Radiation towards load from side wall of FSG as function of frequency*
—o— 11 GHz
- 12 GHz
—●— 13 GHz
---▼--- 16 GHz

The radiation angle from the leaky-wave structure is usually based on calculation of the transverse wavenumber which is approximately found by assuming that the wavenumber along the axis of the structure is very close to that in the closed guide on which the structure is based [3]. Unfortunately this approach breaks down when the apertures in the walls are large and numerous because the axial wavenumber is then not known. This is the case with the FSG. With regards to small perturbations from closed guides, the radiation angle turns out to be (of structures based on rectangular waveguides) the same as the angle of propagation of the two internal plane waves, which may be used to represent the dominant mode. In our FSG the radiated angle is closer to broadside at low frequencies, with the discrepancy becoming smaller as the FSS resonance is reached. According to the transverse resonance method at lower frequencies the FSG appears to have smaller transverse dimensions than at higher frequencies, with the apparent dimensions being the same as the physical dimensions near the FSS resonance. Hence at lower frequencies the guide appears smaller and the wave angle approaches the cutoff (broadside) angle more quickly than in standard guide, accounting for the radiation being closer to broadside.

The radiation from the FSG may also be considered to be to a slow wave, similar to that of a dielectric guided loaded with conducting strips. The surface can be generally treated as an artificial dielectric, see for example [3, 4]. With the element spacing less than a quarter of the operating wavelength, the measured beam swing of the FSG corresponds to that of a

dielectric guide with relative permittivity of near 30 which decreases as the frequency increases.

Conclusions: Strong waveguiding has been demonstrated in a hollow guide made entirely of a frequency selective surface. The structure appears to behave as a leaky-wave structure below the guiding region, and at still lower frequencies supports a wave bound to the structure which contributes to forward guiding. The actual angle of the radiation is related to the angle of propagation of the internal plane waves in a hollow guide. The FSG may also be considered as behaving like an artificial dielectric, whose beam angle can be identified with that expected from a strip loaded dielectric guide.

The forward transmission maximum has associated loss due to non-coincidence of the frequencies of resonance of the broad and narrow walls due to the different local field conditions on each wall. Work is continuing in an attempt to minimise this forward transmission loss and optimise the leakage. A theoretical study based on a vector Floquet mode field expansion as well as a finite array analysis [5], has been initiated to gain further understanding of the guided and radiated fields of the frequency selective guide.

 23rd June 1993

A. J. Robinson, J. C. Vardaxoglou and R. D. Seager (*Department of Electronic and Electrical Engineering, Loughborough University of Technology, Loughborough, Leicestershire LE11 3TU, United Kingdom*)

References

1 ROBINSON, A. J., SEAGER, R. D., and VARDAXOGLOU, J. C.: 'Waveguide with resonant array inserts', *Electron. Lett.*, 1992, **28**, pp. 2122–2123
2 VARDAXOGLOU, J. C., SEAGER, R. D., and ROBINSON, A. J.: 'Realisation of frequency selective horn antenna incited from passive array', *Electron. Lett.*, 1992, **28**, pp. 1955–1956
3 COLLIN, R. E., and ZUCKER, F. J. (Eds.): 'Antenna theory, Part 2' (McGraw-Hill, New York, 1969), Chaps. 18 and 20
4 COLLIN, R. E.: 'Field theory of guided waves' (IEEE Press, 1990), Chap. 12
5 STYLIANOU, A., and VARDAXOGLOU, J. C.: 'Moderate conjugate gradient FFT method for rapid convergence in analysing finite FSS', *Electron. Lett.*, 1992, **28**, pp. 506–508

EFFECTS OF SLOW FADING ON THE PERFORMANCE OF A CDMA SYSTEM

S. Ariyavisitakul

Indexing terms: Fading, Code division, Multiple access, Mobile radio systems

The Letter investigates the issue of uncorrelated multipath fading on uplink and downlink radio channels which impacts the handoff decision quality of slowly moving users in a CDMA system. Simulation results indicate a resulting capacity reduction by as much as 30% when all the users experience quasistationary, single-path Rayleigh fading. This work is targeted toward understanding the traffic capacity and deployment implications to local exchange networks of wireless technology alternatives that could provide access to those networks.

Introduction: Direct-sequence-code-division multiple access (CDMA) techniques have received extensive attention as an alternative digital wireless technology option for mobile and personal communications [1, 2]. Previous capacity analyses of a proposed CDMA approach [2–4] have been based on an ideal handoff model where each user is assumed to communicate with, and thus be power-controlled by, a base station with the largest path gain. The measured path gain is assumed to be determined by distance-dependent path loss and log-normal shadowing. Any measurement error or delay in setting up a new communication path in the fixed wireline network will eventually affect the radio link quality of each user. In reality, handoff decisions are made by individual users based on downlink measurements of pilot signal power. This Letter focuses on the impact of slowly moving users (e.g. pedestrians); for these users, it is difficult to separate slow multipath (Rayleigh) fading from other factors affecting the measured signal variations. The base station chosen by each user based on downlink measurements that include the short-term fading process may not exhibit the maximum path gain on the uplink, because multipath fading on the uplink and downlink is uncorrelated. As a result, these users must transmit at a higher average signal power level, thereby causing an increased amount of uplink interference to all other users, relative to ideal handoff assumed in earlier studies. To study the impact of slowly moving users, we consider a system consisting of quasistationary users only. We simulated the uplink performance of such a system assuming undelayed handoffs and perfect power control based on signal-to-interference ratio (SIR) [3]. This work is targeted toward understanding the traffic capacity and deployment implications to local exchange networks of wireless technology alternatives that could provide access to those networks.

System model: Simulations were performed based on the following assumptions:

(i) The system includes a square grid of base stations with omnidirectional antennas. Users are randomly located in the system with a uniform density of N_u users per base station and are assumed to transmit at a constant information rate without the use of voice activity [2].

(ii) The distance-dependent path loss obeys a fourth power law. Log-normal shadowing with a standard deviation of 10 dB is assumed for pedestrian environments [5].

(iii) Two-branch antenna diversity is assumed on the uplink. The downlink uses only a single antenna because the use of additional RF, IF, and demodulation circuits at the user's radio unit is considered to be impractical.

(iv) The number of equal-average-strength Rayleigh fading paths resolvable (but not necessarily captured) by the receiver, denoted by K_p, is varied as a parameter. Independent Rayleigh fading samples are assigned to individual resolved paths on the uplink and downlink, assuming the same total number of resolved paths on each link. These are superimposed on the large-scale path loss and shadow fading which, however, are perfectly correlated on uplinks and downlinks. The effect of uncaptured energy [6] is also investigated.

(v) SIR-based uplink power control with a normalised maximum power limit $\Lambda = 0$ dB is assumed (see Reference 3 for details). Because a quasistationary situation is assumed, power control can track all the short-term SIR variations due to multipath fading.

(vi) The use of soft handoff [3, 4] between two base stations with a threshold of 6 dB is assumed.

Simulation results: Our performance study is based on 99% required system reliability, i.e. the system capacity is determined by the maximum allowable user density N_u that permits

$$\overline{SIR}_{99\%} = \overline{SIR}_R \tag{1}$$

where $\overline{SIR}_{99\%}$ is the achieved local-mean SIR at the 99th percentile and $\overline{SIR}_R$ is the required local-mean SIR to achieve the desired performance for each radio link. Following Reference 3, we focus on characterising the performance measure η defined as

$$\eta \triangleq \frac{\overline{SIR}_{99\%}}{L/N_u} \tag{2}$$